ChemComm

Accepted Manuscript

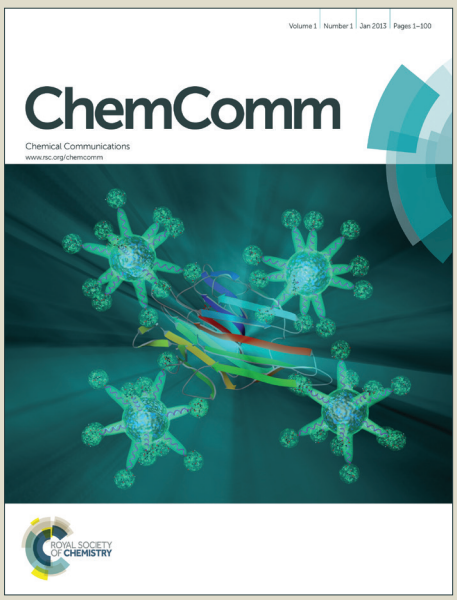

ROYAL SOCIETY OF CHEMISTRY

www.rsc.org/chemcomm

ChemComm

RSCPublishing

COMMUNICATION

Thermally activated polymorphic transition from 1D ribbon to 2D carpet: squaric acid on Au(111)†

Cite this: DOI: 10.1039/xoxxoooooox

Kan Ueji,‡[ab] Jaehoon Jung,‡[a] Junepyo Oh,[a] Kazuo Miyamura[b] and Yousoo Kim*[a]

Received ooth January 2012,
Accepted ooth January 2012

DOI: 10.1039/xoxxoooooox

www.rsc.org/chemcomm

Polymorphic transition from the 1D ribbon to 2D carpet superstructure of squaric acid molecules on Au(111) was achieved through thermally activated process. Our combined STM and DFT study revealed that the molecular arrangements in 1D and 2D superstructures are determined by the stability of their conformational isomers and assembled structures, respectively.

Polymorphic transitions of molecular assemblies on solid surfaces have recently attracted great interest for developing organic-based functional devices. The polymorphic transition has so far been extensively studied on supramolecular assemblies at the liquid-solid interfaces.[1] However, ultrahigh-vacuum (UHV) condition provides different approach to fabricate "solvent-free molecular assembly" and to control its morphology and physical properties.[2] The polymorphic transition of molecular assembly under UHV is, therefore, of importance for gaining fundamental insights into the underlying mechanism based on molecule-substrate and/or intermolecular interactions without involving solvent molecules.[3] Intermolecular interactions such as hydrogen bonding (H-bonding) and van der Waals (vdW) interactions, balanced with molecule-substrate interactions, are generally considered to play an important role in engineering molecular arrangements on solid surfaces.[4] Merz et al. reported the temperature-controlled reversible polymorphic transition in a two-dimensional (2D) molecular crystal of bowl-shaped corannulene on Cu(111) on the basis of the relation between the temperature-dependent population of vibrational modes and intermolecular attractive forces,[2a] and further demonstrated the possibility of selecting a desired assembly structure with intermolecular steric blocking.[2b] Conformational changes caused by thermal annealing can also be utilized to achieve a polymorphic transition on solid surfaces. Matena et al. reported the transition from a H-bonded porous to a close-packed rhombic molecular superstructure on Ag(111), of which the driving force was suggested to be a thermally induced *trans-cis* inversion of the terminal amidic group within the molecule.[2c] However, to the best of our knowledge, only a few studies have been reported on the polymorphic transition under UHV condition with respect to the dimensionality of molecular assembly on solid surfaces, such as via changing the chemical composition[5] or surface coverage[6], despite the importance of structural versatility in designing molecular assembly as a building block for ultimate device miniaturization.

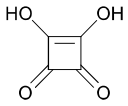

Scheme 1 Squaric acid (3,4-dihydroxycyclobut-3-ene-1,2-dione).

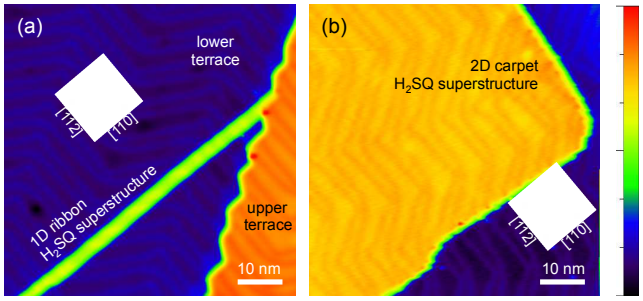

Fig. 1 STM images (65 × 65 nm^2) of (a) as-deposited 1D ribbon (V_s = 500 mV, I_t = 0.25 nA) and (b) 2D carpet H_2SQ superstructure after annealing at ~320 K for 5 min (V_s = 400 mV, I_t = 0.3 nA).

In this Communication, we demonstrate the polymorphic transition from a 1D ribbon to a 2D carpet superstructure of squaric acid (H_2SQ, see Scheme 1 for the structure) molecules on a Au(111) surface through thermally activated process, using scanning tunneling microscopy (STM) and density functional theory (DFT) calculations. Our study revealed that the stability of the conformational isomers and assembled structures is crucial for determining the dimensionality of the 1D ribbon and 2D carpet H_2SQ superstructures, respectively. We here employ the simple H_2SQ molecule as a prototype system that forms a layered structure with strong H-bonding. Electric properties of H_2SQ not only in its molecular crystal[7] but also in its thin film[8] have been reported to be strongly associated with ordering of H-bonds depending on thermal phase transition. In addition, a series of planar oxocarbon acid ($H_2C_nO_n$) molecules has received much attention as electro-active materials.[9]

All the STM images were obtained using a low-temperature

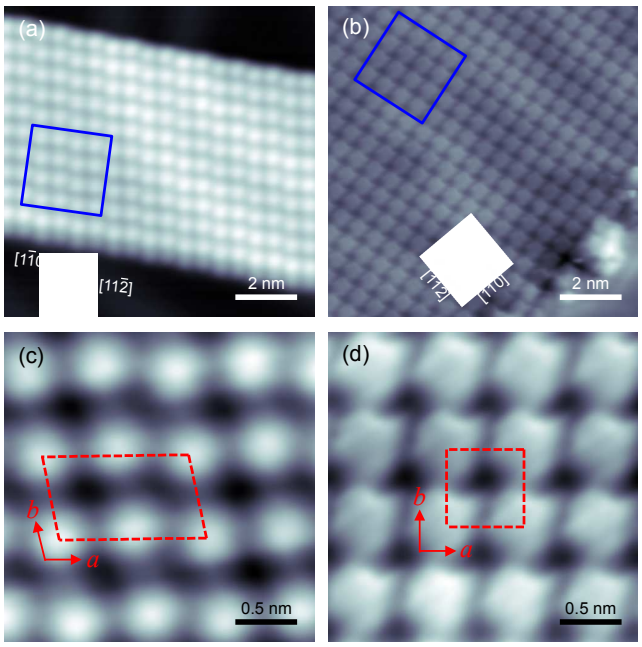

Fig. 2 Molecularly resolved STM images of (a) 1D ribbon (V_s = 250 mV, I_t = 0.3 nA) and (b) 2D carpet (V_s = 25 mV, I_t = 0.3 nA) H_2SQ superstructures on a Au(111) surface. Magnified STM images of blue squares in (a) and (b) are presented in (c) and (d), respectively. Unit cells of both structures are indicated with red-dashed lines.

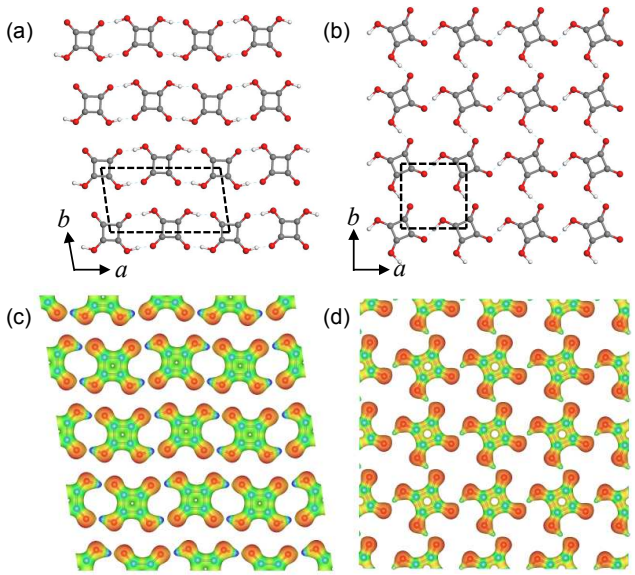

Fig. 3 Optimized structures of (a) 1D ribbon and (b) 2D carpet H_2SQ superstructures (C, gray; H, white; O, red), corresponding to Fig. 2c and 2d, respectively. Unit cells are indicated with black-dashed lines in (a) and (b). Electrostatic potential maps for 1D and 2D superstructures are presented in (c) and (d), respectively. The relative color scale of electrostatic potential maps from red to blue corresponds to negative to positive region on the molecular surface.

scanning tunneling microscope (LT-STM, Oxford Instruments) at 5 K in an UHV chamber, where the base pressure was maintained below 5.0×10^{-11} Torr. Sample cleaning and H_2SQ evaporation were carried out in a preparation chamber. The Au(111) crystal was cleaned by several cycles of argon-ion sputtering (Ar pressure, 3×10^{-6} Torr; energy, 1.5 keV) and annealing at 870 K. H_2SQ (Tokyo Chemical Industry Co., Ltd.) was purified by degassing in a home-built Knudsen cell. H_2SQ molecules were evaporated onto the clean Au(111) surface by heating the Knudsen cell to 490 K. The Au(111) sample was held at room temperature (RT) during the H_2SQ deposition, and then was transferred to the STM chamber for observation.

Fig. 1 shows the STM images of two types of H_2SQ molecular superstructures formed on Au(111). The narrow 1D ribbon superstructure was observed after depositing H_2SQ molecules onto Au(111) at RT (Fig. 1a). We also provided large-scale STM images including several ribbon structures and the histogram of measured ribbon widths in Fig. S1, ESI†. After deposition at RT, we did not observe isolated molecules or small molecular aggregates on the surface, which implies that RT provides sufficient thermal energy for molecular diffusion. Subsequent thermal annealing at ~320 K resulted in a polymorphic transition to the 2D carpet superstructure (Fig. 1b). It should be noted that the polymorphic transition did not involve additional deposition of H_2SQ molecules, despite a significant difference in the local coverage between 1D and 2D superstructures shown in Fig. 1a and 1b. As shown in Fig. 1a, the growth of the 1D superstructure is initiated from the step edge of the Au(111) substrate. The vicinal step edges near the 1D superstructure are not covered by H_2SQ molecules. Whereas the 1D superstructure presents a fully anisotropic morphology with a high length-to-width aspect ratio, the 2D superstructures are close to an isotropic square island with a size of several thousands of nm^2. Although the 1D superstructures look like dominantly aligning along $\langle 1\bar{1}0 \rangle$ on Au(111) (Fig. 1a and Fig. S1, ESI†), there is no apparent periodic coincidence of molecular arrangement with respect to Au lattice. The herring-bone reconstructed Au(111) structure is also clearly seen inside both the 1D and 2D superstructures (see also Fig. 2). These experimental observations indicate that intermolecular interactions between H_2SQ molecules via H-bonding are much stronger than molecule-substrate interactions.

Fig. 2 shows the molecularly resolved STM images, which not only show uniform molecular electronic structures but also provide a view of the detailed molecular arrangements inside the 1D ribbon (Fig. 2a) and 2D carpet (Fig. 2b) superstructures. The blue square regions of Fig. 2a and 2b were enlarged, as shown in Fig. 2c and 2d, respectively. The unit cells indicated by the red-dashed lines reveal the different molecular arrangements, i.e., anisotropic parallelogrammic arrangement (γ = 82±0.1°) for 1D (Fig. 2c) and isotropic square arrangements for 2D (Fig. 2d) H_2SQ superstructures. The unit cell parameter b (6.4±0.3 Å) is longer than half of a (11.6±0.4 Å) by ~0.6 Å, which means that intermolecular interactions in a molecular row along the a-axis are stronger than those between the neighboring rows along the b-axis in the 1D superstructure (Fig. 2c). After annealing, a unit cell of isotropic square lattice ($a = b$ = 6.2±0.2 Å) was observed from the 2D superstructure (Fig. 2d), where side lengths of the unit cell are close to those of 2D H_2SQ sheets in the 3D molecular crystal of the $P2_1/m$ phase (a = 6.143 Å, b = 6.148 Å), as measured by neutron diffraction experiments.[7a] Therefore, our experimental observations indicate that the polymorphic transition by thermal annealing induces a change in the molecular arrangement and dimensionality of the molecular superstructures, according to variations in the intermolecular interactions.

To interpret the experimental results obtained using STM, we carried out extensive periodic DFT calculations with a variety of molecular arrangements (see ESI† for computation details and Fig. S2-S4, ESI† for initial molecular arrangements). We used the DFT-D2 method[10] to fully consider the intermolecular interactions, including the vdW forces. Based on the incommensurate molecular arrangement for both 1D and 2D H_2SQ superstructures on Au(111), indicating weak molecule-substrate interaction, we performed DFT

calculations considering only the molecular configurations without substrate, in which the planarity of molecular assembly was kept by symmetry constraints. The optimized structures corresponding to the 1D ribbon (Fig. 2c) and 2D carpet (Fig. 2d) H_2SQ superstructures are presented in Fig. 3a and 3b, respectively. Although the influence of Au(111) on the molecular arrangement was not involved in the DFT calculations, the geometric information of the optimized superstructures agrees fairly well with the experimental values (see Table S1, ESI†), which implies that the polymorphism of H_2SQ on Au(111) does not significantly depend on the molecule-substrate interaction. Our calculations revealed that the 2D superstructure is more stable than the 1D superstructure by 0.12 eV per one H_2SQ molecule (see Fig. S5, ESI†). Therefore, the polymorphic transition from the 1D to 2D superstructure by thermal annealing, as observed in our STM experiments, can be clearly explained by the higher stability of 2D carpet superstructure. Interestingly, according to the computational results, the two H_2SQ superstructures on Au(111) are composed of different conformational isomers (Fig. 3a and 3b). As described in the ESI†, an isolated H_2SQ molecule has five conformational isomers depending on the relative position of the two H atoms, in which the most stable two isomers are **ZZ** (C_{2v}) and **EZ** (C_s) (see Table S2, ESI† for the optimized structures and relative energies of the five H_2SQ isomers). Our DFT-D2 calculations showed that, in the gas phase, the **ZZ** isomer is more stable than the **EZ** isomer by 0.11 eV (2.64 kcal/mol), which is in good agreement with previous theoretical reports.[11] Fig. 3 shows that the less stable 1D structure compared to the 2D structure consists only of **ZZ** isomers, which are more stable than **EZ** isomers. In contrast, after annealing, the 2D structure is composed of only **EZ** isomers. These results indicate that different driving forces induce the formation of the two superstructures. The initial formation of the 1D superstructure at RT is determined by the relative monomeric stability among the H_2SQ isomers in the gas phase, and the polymorphic transition from the 1D to 2D superstructure by annealing can be explained by a change in the overall stabilization mechanism from the stability of individual monomers to the stability of the assembled structure. In addition, it is spontaneously expected that the annealing process provides thermal energy required for conformational change as well as collective diffusion of molecules on the surface, considering the relative stability of two isomers.

The main intermolecular interaction in both superstructures can be considered to be H-bonding (Fig. 3). The H-bonding distance within the 2D molecular arrangement is calculated to be 1.33 Å, which is considerably shorter than that in the 1D superstructure (1.43–1.47 Å). Our DFT calculations, therefore, indicated that the polymorphic transition from 1D to 2D superstructure requires the rearrangement of H_2SQ molecules accompanied with the conformational change from **ZZ** to **EZ** isomers, although the detailed dynamic feature of the polymorphic transition, such as transition state and molecular diffusion on the surface, was not fully addressed. As a consequence, the 2D carpet superstructure achieves the more effective intermolecular H-bonding network compared to the 1D ribbon superstructure, during the annealing process. In addition to H-bonding interactions, we can consider vdW interactions within the 1D molecular arrangement (Fig. 3a), where the neighboring molecular rows, entangled by H-bonding along the *a*-axis, are interlocked by the vdW interactions along the *b*-axis. To study the influence of intermolecular interactions on a molecular arrangement in more detail, we plotted the electrostatic potential maps for both the 1D and 2D superstructures in Fig. 3c and 3d, respectively. While attractive H-bondings are found in the 2D superstructure in an isotropic manner (Fig. 3d), electrostatic repulsion between the neighboring molecular rows in the 1D superstructure (Fig. 3c) causes a gradual shift in the position of the molecular rows along the *a*-axis, which causes not only the distortion of the rectangular arrangement but also the alternative displacement of the molecular center from the axis of the molecular rows. In order to investigate the variation in electronic property due to polymorphic transition, we examined the redistributions of electron density during the formation of 1D and 2D superstructures (see Fig. S6, ESI†). We found clear anisotropic and isotropic polarization of electron density for 1D and 2D molecular arrays, respectively, mostly in the intermolecular space where H-bondings form between adjacent H_2SQ molecules. The geometry of four-membered ring is also be influenced by the transition, and thus the deviation of C-C bond lengths in 2D superstructure becomes smaller, i.e., more highly π-conjugated, than that in 1D superstructure (see Fig. S7, ESI†). The H-bonding network and π-conjugated framework in H_2SQ molecular crystals has been known to be important for manifesting the electric properties.[7, 11a] Therefore, our findings suggest that the polymorphic transition from the 1D to 2D superstructure presents an opportunity to achieve a new type of selectivity in the directional electric properties of H_2SQ polymorphs towards novel functional devices.

To summarize, we have demonstrated the thermally activated polymorphic transition from 1D ribbon to 2D carpet superstructures using H_2SQ molecules on Au(111) in UHV condition through STM experiments combined with DFT calculations. We found that the molecular arrangements in the 1D ribbon and 2D carpet superstructures are determined by the stability of the conformational isomers and assembled structures, respectively. Our study provides a new platform for developing highly controlled electric devices.

We are grateful to the computational resources of the RIKEN Integrated Cluster of Clusters supercomputer system. K.U. and J.J. acknowledge the Junior Research Associate and Foreign Postdoctoral Researcher program of RIKEN, respectively, for financial support.

Notes and references

[a] *Surface and Interface Science Laboratory, RIKEN, 2-1 Hirosawa, Wako, Saitama 351-0198, Japan. Fax: +81 48 467 1945; Tel: +81 48 467 4073; E-mail: ykim@riken.jp*

[b] *Department of Chemistry, Faculty of Science, Tokyo University of Science, 1-3 Kagurazaka, Shinjuku, Tokyo 162-8601, Japan.*

† Electronic Supplementary Information (ESI) available: Unit cell parameters of 1D ribbon and 2D carpet H_2SQ superstructures, computation details, relative energies of five H_2SQ geometric isomers in the gas phase, initial periodic molecular arrangements for geometry optimizations, eight optimized stable superstructures, and electron density difference maps for 1D and 2D superstructures. See DOI: 10.1039/c000000x/

‡ These authors contributed equally to this work

1. (a) R. Gutzler, T. Sirtl, J. F. Dienstmaier, K. Mahata, W. M. Heckl, M. Schmittel and M. Lackinger, *J. Am. Chem. Soc.*, 2010, **132**, 5084; (b) A. Jahanbekam, S. Vorpahl, U. Mazur and K. W. Hipps, *J. Phys. Chem. C*, 2013, **117**, 2914; (c) M. O. Blunt, J. Adisoejoso, K. Tahara, K. Katayama, M. Van der Auweraer, Y. Tobe and S. De Feyter, *J. Am. Chem. Soc.*, 2013, **135**, 12068.
2. (a) L. Merz, M. Parschau, L. Zoppi, K. K. Baldridge, J. S. Siegel and K.-H. Ernst, *Angew. Chem. Int. Ed.*, 2009, **48**, 1966; (b) L. Merz, T. Bauert, M. Parschau, G. Koller, J. S. Siegel and K.-H. Ernst, *Chem. Commun.*, 2009, 5871; (c) M. Matena, A. Llanes-Pallas, M. Enache, T. Jung, J. Wouters, B. Champagne, M. Stöhr and D. Bonifazi, *Chem. Commun.*, 2009, 3525.
3. (a) T. Takami, U. Mazur and K. W. Hipps, *J. Phys. Chem. C*, 2009, **113**, 17479; (b) T. Sirtl, W. T. Song, G. Eder, S. Neogi, M. Schmittel, W. M. Heckl and M. Lackinger, *ACS Nano*, 2013, **7**, 6711.
4. (a) S. De Feyter and F. C. De Schryver, *Chem. Soc. Rev.*, 2003, **32**, 139; (b) J. V. Barth, G. Costantini and K. Kern, *Nature*, 2005, **437**, 671; (c) H. W. Kim, J. Jung, M. Han, S. Lim, K. Tamada, M. Hara, M. Kawai, Y.

Kim and Y. Kuk, *J. Am. Chem. Soc.*, 2011, **133**, 9236; (d) J.-H. Kim, K. Tahara, J. Jung, S. De Feyter, Y. Tobe, Y. Kim and M. Kawai, *J. Phys. Chem. C*, 2012, **116**, 17082; (e) T. K. Shimizu, J. Jung, T. Otani, Y.-K. Han, M. Kawai and Y. Kim, *ACS Nano*, 2012, **6**, 2679.
5. T. Yokoyama, S. Yokoyama, T. Kamikado, Y. Okuno and S. Mashiko, *Nature*, 2001, **413**, 619.
6. C. Iacovita, P. Fesser, S. Vijayaraghavan, M. Enache, M. Stöhr, F. Diederich and T. A. Jung, *Chem. Eur. J.*, 2012, **18**, 14610.
7. (a) D. Semmingsen, F. J. Hollander and T. F. Koetzle, *J. Chem. Phys.*, 1977, **66**, 4405; (b) F. J. Hollander, D. Semmingsen and T. F. Koetzle, *J. Chem. Phys.*, 1977, **67**, 4825; (c) N. Dalal, A. Klymachyov and A. Bussmann-Holder, *Phys. Rev. Lett.*, 1998, **81**, 5924.
8. T. Shimada, I. Sugiura and K. Saiki, *Jpn. J. Appl. Phys.*, 2008, **47**, 1422.
9. S. Horiuchi, Y. Tokunaga, G. Giovannetti, S. Picozzi, H. Itoh, R. Shimano, R. Kumai and Y. Tokura, *Nature*, 2010, **463**, 789.
10. S. Grimme, *J. Comput. Chem.*, 2006, **27**, 1787.
11. (a) C. Rovira, J. J. Novoa and P. Ballone, *J. Chem. Phys.*, 2001, **115**, 6406; (b) M. M. Montero-Campillo, A. M. Lamsabhi, O. Mó and M. Yáñez, *J. Mol. Model.*, 2013, **19**, 2759.

